PERGAMON

Journal of Structural Geology 22 (2000) 693–711

JOURNAL OF STRUCTURAL GEOLOGY

www.elsevier.nl/locate/jstrugeo

Relationship between polarity of extensional fault arrays and presence of detachments

S.A. Stewart*, J.D. Argent

Amerada Hess Ltd, 33 Grosvenor Place, London SW1X 7HY, UK

Received 25 January 1999; accepted 16 November 1999

Abstract

Extensional fault arrays are often dominated by a single fault vergence, forming 'domino' fault blocks. The polarity of faults can be defined as synthetic or antithetic in relation to the overall shear sense across the fault system. Observations of the geometry of a number of field examples of extensional fault arrays vs. the lithologies (as a proxy for strength profile) show that synthetic extensional arrays from the North Sea and Bristol Channel Basin detach on salt layers, whereas examples of antithetic arrays from the North Sea are found to pin out downwards and no basal detachment is present. In the Sacramento Mountains core complex of the Basin and Range, the major low-angle detachment fault post-dates antithetic shears that evolved at mid-crustal level and are preserved in the granitic footwall. These antithetic shears were cut by the main low-angle detachment, whose hanging wall disintegrated into an array of synthetic faults. The kinematics of synthetic vs. antithetic arrays dictate that faults within synthetic arrays must branch onto a basal detachment, whereas faults within antithetic arrays may die out downwards. Therefore, the results emphasise that fault polarity in domino arrays may be related to the boundary conditions of the fault blocks and therefore may be diagnostic of the strength profile of the faulted stratigraphy.

1. Introduction

Arrays of normal faults occur at all scales from crustal to hand specimen. In some cases, there is a mixture of fault facing directions. In nature and experiment, however, it is common to observe a dominant fault polarity in the array, giving 'domino' style fault blocks. The terms 'synthetic' and 'antithetic' can only be used when related to some reference frame, for example, the dip of regional bedding or some nearby major fault structure. In addition to specifying the reference frame, one must also specify whether the terms 'synthetic' and 'antithetic' refer to the domino faults themselves, or the sense of rotation of the domino fault blocks, as the choice gives rise to opposite use of the nomenclature (Fig. 1a). Those working on the internal kinematics of shear zones tend to use the sense of rotation of the domino fault blocks, or equivalent structures (e.g. Jordan, 1991), whereas research on outcrop or seismic scale domino normal fault arrays tends to use the sense of shear on the domino faults (e.g. Axen, 1988). Selecting a reference frame against which to define synthetic and antithetic is not straightforward, as a fault array may or may not be confined to a given stratigraphic interval or layer, and since it is assumed here that as the presence of detachments is not initially known, the relative sense of movement of the layers above and below the domino blocks may not be known either. We adopt a convention based on the facing of domino faults relative to the dip of a medial line drawn through the domino fault blocks at the time of faulting. For example, in the case of a domino fault array forming

* Corresponding author.
E-mail address: simon.stewart@hess.com (S.A. Stewart).

0191-8141/00/$ - see front matter
PII: S0191-8141(00)00004-3

as a result of gravity gliding precipitated by regional tilt, this nomenclature follows Axen (1988).

Fault polarity is discussed here in terms of the strength profile of the multilayer and the resulting boundary conditions that are imposed on fault blocks, i.e. in the case of domino arrays in sedimentary basins, relating the fault style to the stratigraphy itself. This paper begins with a short review of published work relevant to domino fault arrays, followed by an explanation of the suggested relationships between fault array polarity and fault block boundary conditions/stratigraphy. These relationships are then explored with reference to a number of field examples that are examined in an attempt to build confidence in the proposed relationships so that they might be used to deduce the presence or otherwise of a basal detachment in a seismically imaged domino fault array where the lithologies were unknown.

2. Review

Many textbooks review the principle of 'Andersonian' conjugate shears developing at some angle to the principal compressive stress (e.g. Price and Cosgrove, 1990). The geometrical problems posed by synchronous conjugate faults (Horsfield, 1980; Watterson et al., 1998) are by definition not an issue in domino fault arrays, nor in detachment systems, where the point of intersection tends to be at the base of the sliding layer (e.g. Childs et al., 1993).

Arrays dominated by a single polarity are particularly common in gravity glide systems, which occur in

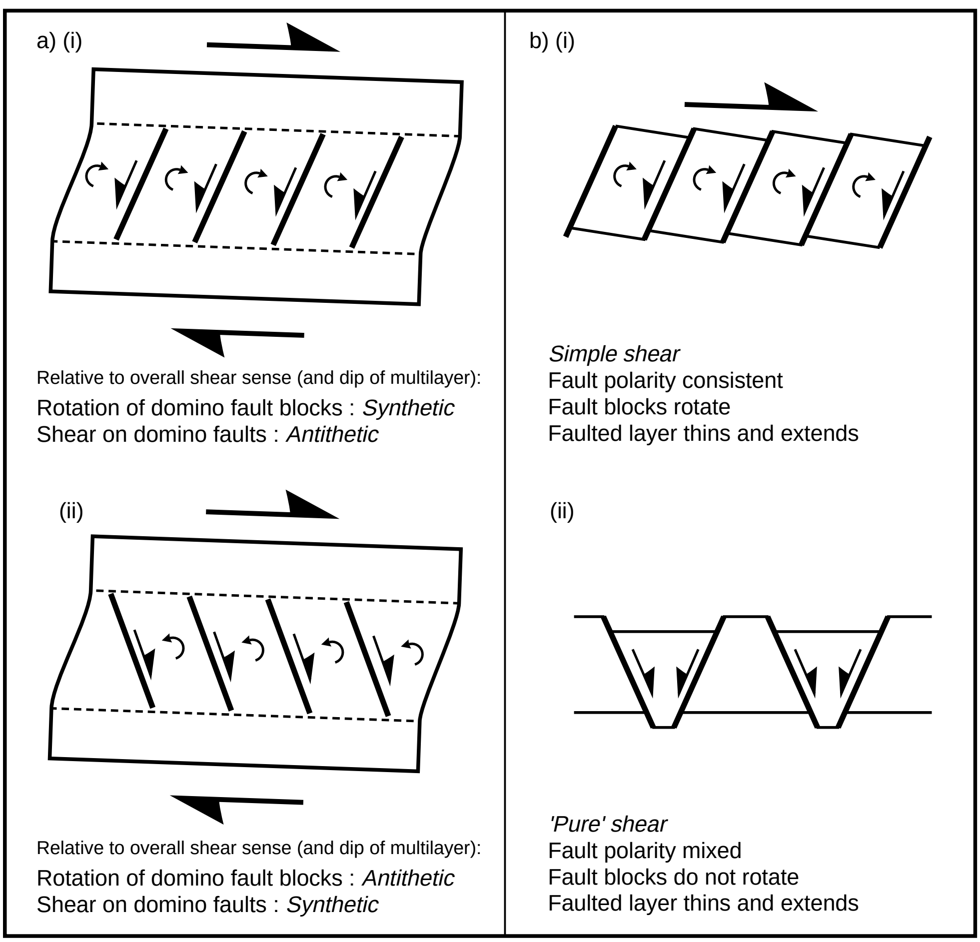

Fig. 1. (a) Defining the terms 'synthetic' and 'antithetic'. If the reference frame is the overall sense of shear on a multilayer, (e.g. as induced by gravity gliding resulting from regional tilt), the choice of synthetic or antithetic to describe the structures within the domino fault zone depends on whether one refers to the sense of shear on the domino faults, or the sense of rotation of the domino fault blocks. Workers studying shear zones prefer the sense of rotation of the domino blocks whereas mappers studying seismic or outcrop scale structures tend to use the sense of shear on the domino faults. These examples are for illustrative purposes only—model a(ii) would require detachments to be present along the dashed lines to be kinematically valid. (b) Illustration of domino faults vs. conjugate normal faults in the context of simple and pure shear. In this idealised view, domino faults accommodate simple shear (i), conjugate faults do not (ii).

tilted multilayers, and fault polarity research has tended to concentrate on these systems. Gravity gliding occurs in tilted stratigraphy and is driven by the body weight of a layer sliding upon a relatively weak layer, or 'detachment' (Price and Cosgrove, 1990). An important aspect of gravity glide systems is that the domino fault arrays may form in layers that are initially isotropic, unlike basement-involved extensional faulting, which often involves reactivation of planes of weakness or anisotropy (Van Wees et al., 1996). Early models of domino normal faults were produced in sandbox models that had a stretching base (e.g. Mandl, 1987; Vendeville et al., 1987; McClay 1990). The domino fault arrays produced in these models were influenced by a shear stress on the base of the faulting layer that was not necessarily representative of that present in gravity glide systems (Mandl, 1987). More recent apparatuses allow an upper layer to gravity glide downslope upon a ductile layer (e.g. Maudit et al., 1997). These models are less prone to developing domino faults during the first increments of extension, when conjugate pairs are common, as Mandl (1987) (p. 313) predicted. The models show, however, that a preferred fault facing develops (usually synthetic) as the ductile layer thins, so the selection of a dominant facing is related to the degree of coupling across the ductile layer (Maudit et al., 1997). The coupling is inversely proportional to the thickness of the ductile layer, which decreases during extension. The mechanical explanation for the selection of synthetic faults is a vexed issue that is not pursued here—discussions of interactions between normal stress, shear stress and fracture orientation are given by Mandl (1988) (pp. 54–87 and 312–317) and Price and Cosgrove (1990) (pp. 226–239).

Numerous examples of natural domino fault arrays have been published, including thick-skinned/basement-involved systems (e.g. Jackson and White, 1989) and thin-skinned/detachment systems (e.g. Diegel et al., 1995; Mohriak et al., 1995; Morley and Guerin, 1996). The thin-skinned examples of domino systems are usually gravity glide systems associated with regional tilt and are particularly prevalent in the circum-Atlantic salt basins. The reason for the dominance of fault facing in these systems is rarely considered beyond intuitive assumptions that detached faults 'ought' to face downdip, and reference is often made to the published analogue experiments mentioned above (e.g. Mohriak et al., 1995). Real examples of thin-skinned fault systems, which have developed under the influence of very low regional tilt, or gravity spreading, often show mixed fault facing, giving horst and graben systems (Fig. 1b; e.g. Trudgill and Cartwright, 1994).

Another issue affecting the study of seismic-scale domino extensional fault arrays is the combined effect of fluctuation in regional dip and exhumation, which can make it difficult to determine regional dip direction at the time of domino fault growth.

The concepts and terminology coined in field and analogue studies of strike slip faults can be employed to various degrees in the study of extensional domino fault systems. Studies of strike slip systems emphasise the geometrical evolution of domino fault systems due to rotation of fault blocks and their bounding faults (Freund, 1974; Naylor et al., 1986; Sylvester, 1988; Woodcock and Schubert, 1994).

3. Relationship between fault polarity and strength profile

The kinematics of synthetic and antithetic fault arrays in inclined multilayers, illustrated by end-member cases of multilayers with and without a detachment, are illustrated on Fig. 2. The purpose of this section is not to develop a mechanical model for preferential fault polarity, but to examine the relationship between kinematics and the strength profile of the multilayer. It is assumed here that the footwall of the system (the layer below the domino array and any associated detachment) does not deform.

3.1. No basal detachment (Fig. 2a)

The faults pin downwards and upwards, although the kinematics would be the same if the faults reached the free upper surface of the multilayer. The kinematics are also independent of whether the lower layer stretches (via, say, pure shear). The key feature of this case is that the fault blocks are continuous with the underlying and overlying layers and are 'pinned' to them. Internal shear in 'soft' dominoes is documented in field and seismically imaged examples (e.g. Faure and Chermette, 1989; Walsh et al., 1996; Ferrill et al., 1998; Hesthammer and Fossen, 1998). The synthetic case (Fig. 2a) involves movement of the domino fault blocks, together with any upper layer, updip, which is incompatible with gravity slip, so this case can be ruled out as kinematically inadmissible during extensional faulting. On the other hand, the antithetic case allows the fault blocks and upper layer to move some distance downdip, which is compatible with gravity sliding. The antithetic faults depicted in Fig. 2(a) can only accommodate a small amount of downdip movement—as the fault blocks rotate, the normal stress component on the fault planes increases, as does the amount of deformation within the fault blocks. Further downslope movement requires new faults. These new faults could be similar to the initial set (Nur et al., 1986) or could activate the rotated layering (e.g. bedding) within the fault blocks as P-shears

(Freund, 1974; Davison, 1989; Ferrill et al., 1998). P-shears formed in this way could ultimately link up to form a low angle detachment, with beheaded remnants of the original antithetics fossilised in the footwall. Application of this model to a Basin and Range field example is discussed later.

The faulted layer in the antithetic case is not necessarily sufficiently 'weak' to be described as a detachment, but it can be regarded as a 'shear zone' in the multilayer.

3.2. Basal detachment (Fig. 2b)

In this case, the normal faults merge downwards on to a basal detachment that is comprised of some weak lithology, which in sedimentary basins could be salt, shale or overpressured sand (Morley and Guerin, 1996). The fault blocks can slide down the detachment layer, so the amount of extension at the toe of the system equals the sum of individual fault heaves within the fault array (in the absence of volumetric contraction). This cumulative extension would have to be balanced downdip by some mechanism such as basement-involved extension or thin-skinned shortening at the toe of the gravity slide. A key feature of displacement across the detachment increasing downdip is that, in the absence of an upper detachment to the fault system, any upper layer would have to stretch, so it is much easier for this kind of fault system to develop if the faults reach the free upper surface of the multilayer. In the synthetic case, although the fault blocks rotate updip, in the opposite direction to the dip of the multilayer, synchronous motion of the fault block keel along the detachment ensures that the fault block as a whole is sliding downdip. The synthetic and antithetic cases both involve downdip movement of the fault blocks and are compatible with gravity gliding.

Only one domino fault scenario out of the four examined here can be regarded as being unlikely on

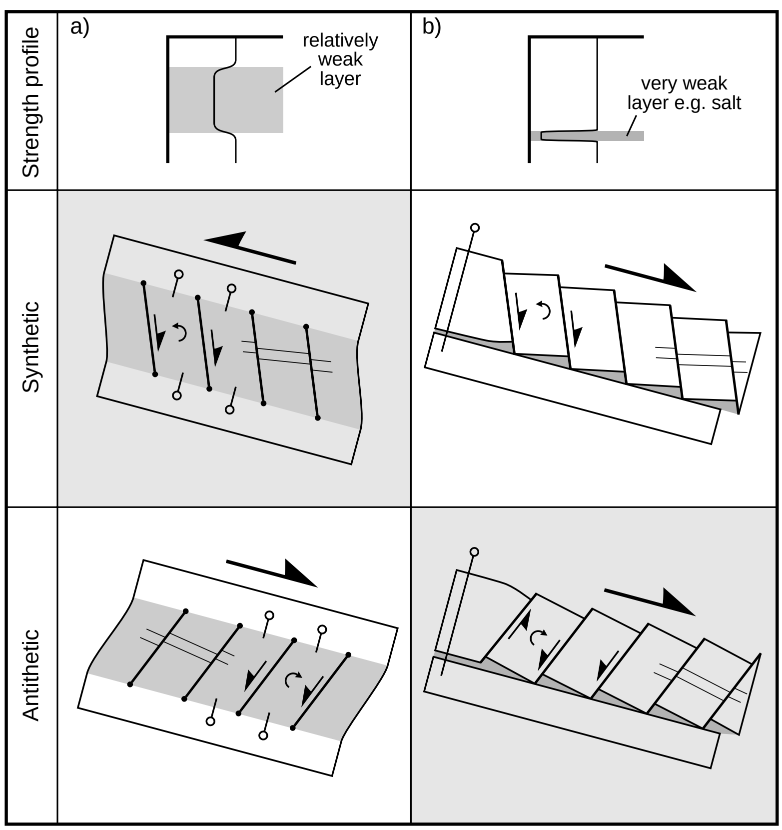

Fig. 2. Illustration of synthetic and antithetic fault polarities in terms of multilayers/stratigraphies where there is no 'detachment' present (a) and there is a detachment present (b). Favoured combinations are shown without shading. The models are shown tilted to imply a clockwise sense of overall shear in each case, as would be induced by gravity gliding resulting from this tilt. In the no detachment, synthetic case (a), this fault array is kinematically incompatible with clockwise shear, and it is concluded that antithetic arrays are preferentially selected in the case where the fault blocks are continuous with the layers above and below. Where the detachment is present, both synthetic and antithetic cases are kinematically compatible with the overall sense of shear, but natural examples usually show that the synthetic case is preferentially selected. So for a given overall sense of shear, synthetic faults indicate the presence of a detachment, antithetic faults indicate that no detachment is present.

the basis of kinematic admissibility (synthetic, no basal detachment). However, as discussed earlier, the mechanics of domino systems appear to mitigate against a further possibility (antithetic, basal detachment), leaving synthetic and antithetic arrays to characterise multilayers with and without a basal detachment, respectively (Fig. 2). A number of field examples are now examined in order to further examine the relationship between multilayer strength profile and fault facing direction.

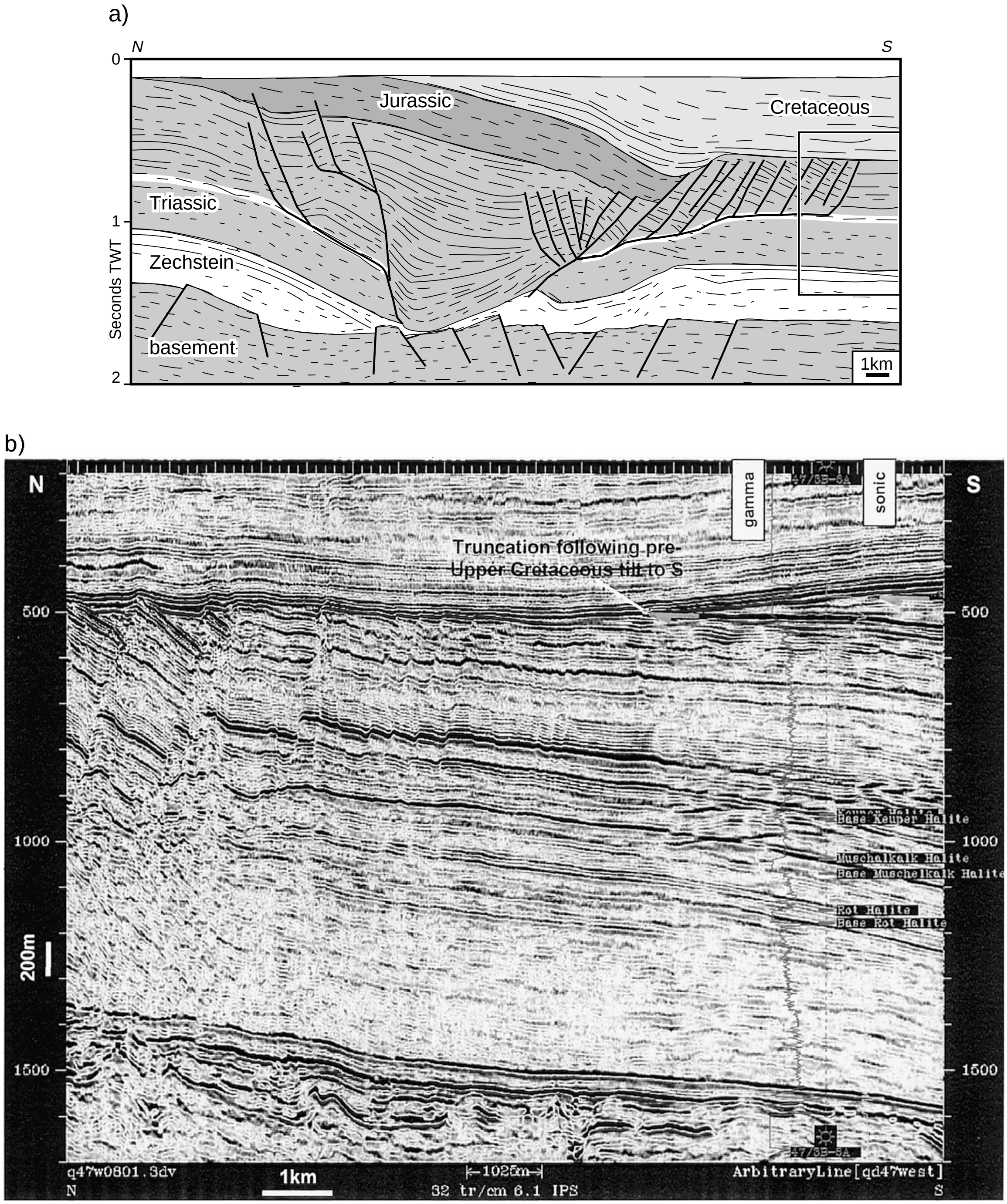

Fig. 3. Domino fault array imaged on time-migrated 3D seismic data, southern North Sea. (a) Geoseismic section (after Stewart et al., 1996) illustrates the context of the seismic section (b) (location on inset box) with respect to a major graben system to the north. An intra-Triassic salt layer (Röt Halite) is marked as a white stripe. Vertical exaggeration of seismic section approximately ×2.5. The domino fault blocks affect the Triassic. Intra Triassic salts are labelled in the well. Note the tilt of Triassic strata to the south dates from pre-Upper Cretaceous regional tilt. Accommodation of extension across this array by the graben to the north is discussed in the text.

4. Synthetic domino array examples

4.1. Southern North Sea

Fig. 3 illustrates a synthetic domino fault array from the southern North Sea. This fault array developed during the Jurassic and consists of extensional faults that sole out in the Triassic section. The faults all detach on Triassic salt, but at progressively shallower levels of décollement with distance away from a major basement fault, which lies to the north (Fig. 3; Stewart et al., 1996, 1997). Due to the post-faulting, pre-Cretaceous erosion, it is not possible to determine whether the faults died out upwards. Displacement across the faults is relatively consistent along the preserved length of the fault strands, with significant displacement still visible at the base of the fault blocks, showing that (in the absence of volumetric contraction within the fault blocks) extension has been transferred along the basal detachment. The area from which Fig. 3 was taken was tilted to the south at some point during the Jurassic–Lower Cretaceous, an event recorded by the unconformity at base Upper Cretaceous (Fig. 3). That tilt resulted in the appearance of the fault array as being antithetic with respect to present-day dip at Triassic level. However, northerly tilt of the area at the time of fault array evolution is illustrated by regional 2D seismic lines that show the domino array linking northwards to a major graben (Fig. 3; Stewart et al., 1996). Extension across this graben balanced that across the domino array.

4.2. Bristol Channel Basin, UK

A second example of a domino fault array is exposed onshore on the south margin of the Bristol Channel Basin (Fig. 4a,b; Dart et al., 1995; Stewart et al., 1997). The faults shown in Fig. 4(b) affect a lower Jurassic section of limestones and shales. This Jurassic section rests on Triassic gypsiferous muds. These muds are heavily sheared at outcrop, and pass downwards into a halite horizon, that has been drilled locally (Fig. 4c) and is interpreted here to be the detachment. The variation in structural style with lithology in the Triassic–Jurassic of this area can be likened to the brittle–brittle/ductile–ductile transitions associated with crustal scale fault structures (Fig. 4c). The rotation of the domino fault blocks makes it difficult to determine the 'regional' dip of the multilayer, but seismic data acquired offshore show that the present day dip of the Central Bristol Channel Fault hanging wall multilayer is over 10° to the north (Fig. 4d; Brooks et al., 1988; Dart et al., 1995).

4.3. Moray Firth Basin, UK vs. Angola

A further example of synthetic domino fault blocks gliding on evaporite detachments is shown in Fig. 5. Fig. 5(a) is from the Buchan area in the Moray Firth, North Sea. Here, the detachment is Permian (Zechstein) salt and the dominoes evolved when the main basement fault events tilted the salt layer during the late Jurassic. These dominoes are very similar in style to those seen offshore west Africa (e.g. Fig. 5b, after Duval et al., 1992).

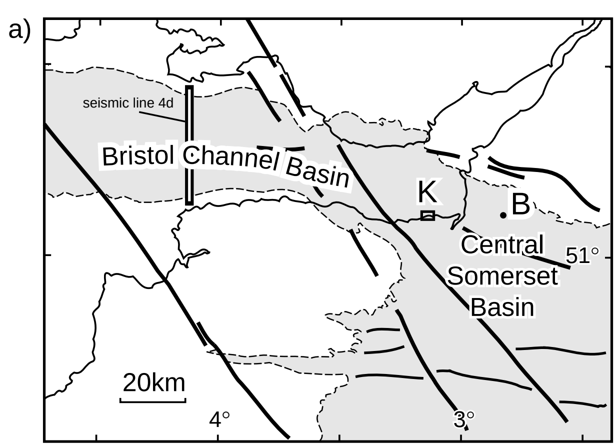

Fig. 4. Domino faults in the Bristol Channel Basin, UK. (a) Location map showing distribution of Triassic evaporites (shaded), Burton Row borehole (B), coastal exposures at Kilve (K) and location of the seismic example. (b) Photograph and line interpretation of domino fault blocks in cliff section at Kilve. (c) Burton Row borehole lithology log, wireline logs, stratigraphy, and interpretative structural style 'log'. (d) Seismic section across the Bristol Channel, showing the northerly tilt of the Mesozoic section into the southerly dipping Central Bristol Channel Fault Zone. Vertical exaggeration approximately ×8. This basement fault soles on to lower-angle, intra Devono-Carboniferous reflectors below the Mesozoic basin.

5. Antithetic domino array examples

5.1. North Sea Tertiary

Extensional fault arrays that are genetically antithetic to multilayer dip are rarer at seismic scale than synthetic arrays. The Tertiary section of the North Sea Basin contains regional, layer-bound fault arrays. These fault arrays often contain a variety of strikes and define polygonal fault blocks (Cartwright and Lonergan, 1996). The polygonal pattern is sensitive to external influences, for example the faults can align with the trends of underlying, differentially compacting sand-filled channels (Jenssen et al., 1993). The displacement on each fault reduces from maximum in the centre of the fault to seismically irresolvable displacement at the deepest part of the fault (Cartwright and Lonergan, 1996). These displacement profiles contrast with those that characterise faults branching onto a basal detachment and indicate that there is no layer-parallel slip between the rocks within the fault blocks and the layers above and below. Around the margins of the North Sea basin there are large (100s of km^2) domains where the fault strikes align parallel with the basin margins. In these domains, the faults consistently face updip, away from the centre of the basin

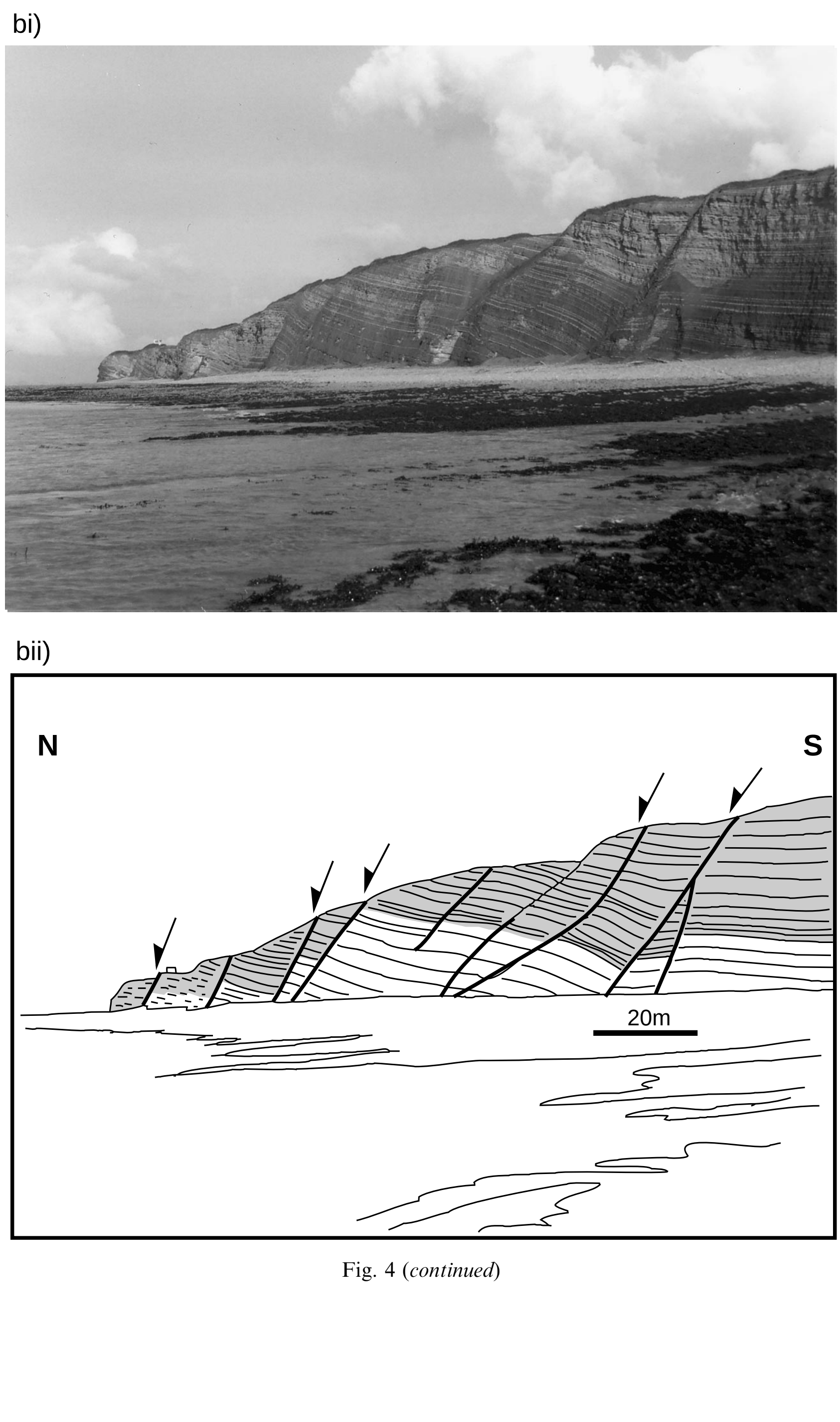

Fig. 4 (*continued*)

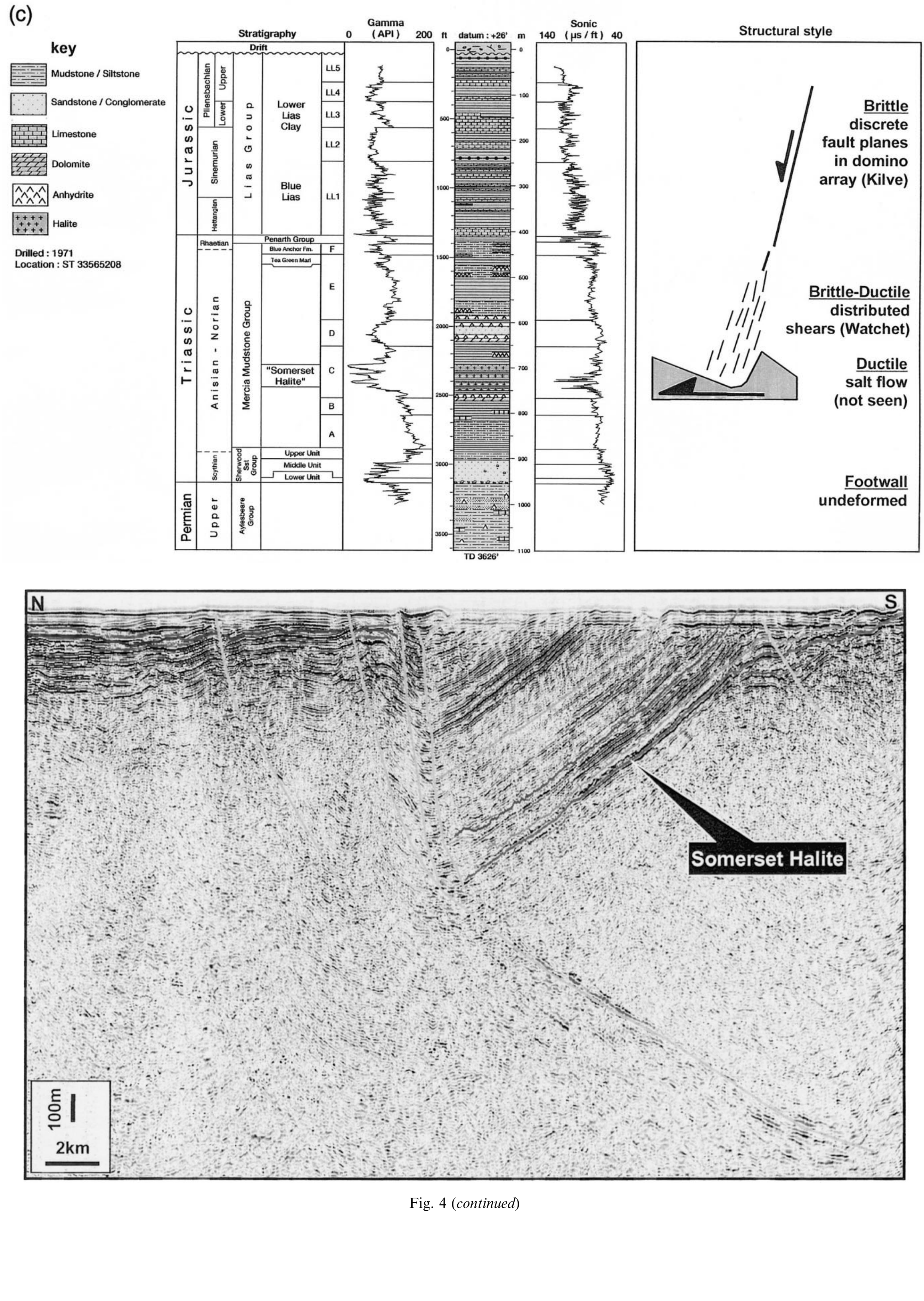

Fig. 4 (*continued*)

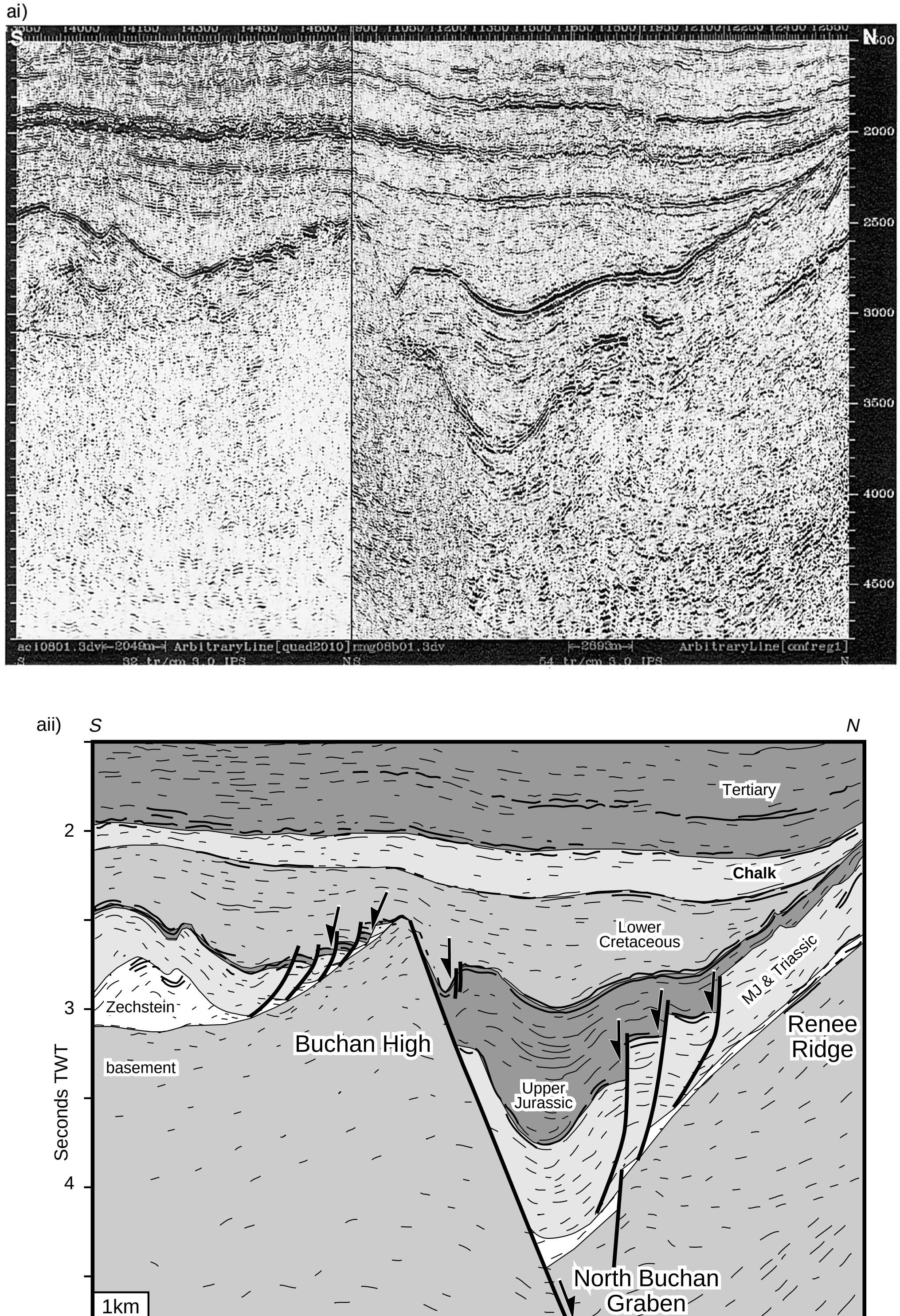

Fig. 5. (a) Seismic section and geoseismic interpretation through the Buchan Graben, Outer Moray Firth, UK. This section spans the original margin of the Permian salt basin. The depositional thickness of salt at the south end of the section is >1 km, but c. 100 m of carbonates and anhydrites constitute the equivalent interval at the north end of the section. The main phase of basement faulting occurred in the late Jurassic. Movement of the Triassic and Jurassic section continued until the end of the Jurassic. This included slip of the cover southwards from the Buchan High. In this section a synthetic array of domino fault blocks can be seen on the dip slope of the Buchan High. Extension across these faults is partly balanced by shortening across a salt pillow-cored anticline visible at the south end of the section. (b) Synthetic fault blocks sliding oceanwards on Albian salt on the passive margin offshore Angola, after Duval et al. (1992).

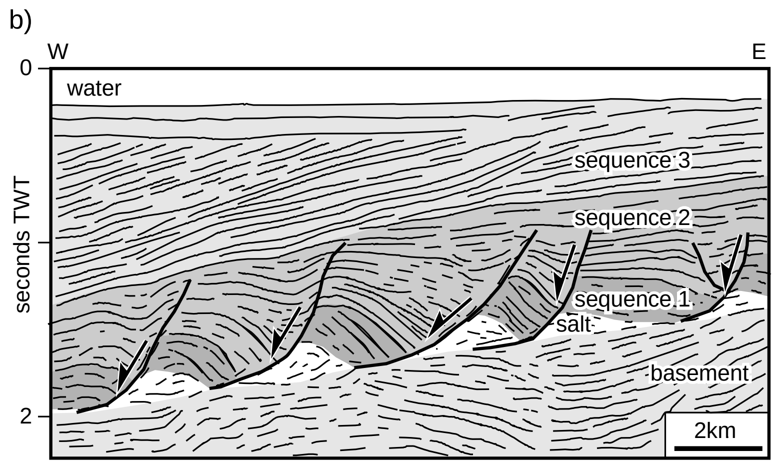

Fig. 5 (*continued*)

(Fig. 6a,b). Studies of Tertiary sediment accommodation space in the North Sea show that regional tilt towards the basin centre evolved consistently from the end of the Cretaceous until the present day (Liu and Galloway, 1997), confirming the interpretation of these faults as antithetic domino arrays. A proposal that the Tertiary fault arrays were entirely the result of gravity gliding by Higgs and McClay (1993) was discounted when large tracts of polygonal fault blocks were identified on 3D seismic data (Cartwright and Lonergan, 1996). However, it appears quite possible that gravity gliding was locally responsible for preferentially selecting fault trend and facing.

5.2. Analogue model

Models of extensional faults by Fossen and Gabrielsen (1996) showed that where a relatively homogeneous layer was subjected to layer parallel shear in an analogous situation to gravity slip, the shear was initially accommodated by an antithetic fault array within the layer (Fig. 7).

5.3. Basin and Range

Arrays of extensional fractures antithetic to the general shear direction have been identified in the footwalls of large-scale, low-angle extensional faults of the type that are associated with metamorphic core complexes (Reynolds and Lister, 1990; Higgs et al., 1991; Fletcher et al., 1995; Pease and Argent, 1999). These antithetic extensional fractures are described here in the context of a new evolutionary model for large-scale, extensional faults, that we offer here as a contribution to the extensive literature on this subject (e.g. Lister and Davis, 1989; Axen, 1992; Wernicke, 1995; Axen and Bartley, 1997). The antithetic shears described here are associated with the Sacramento Mountains core complex, located within the Colorado River Extensional Corridor (Fig. 8a; Howard and John, 1987). This is a belt of extreme mid-Tertiary extension accommodated on a series of northeasterly dipping, regional-scale normal faults that initiated and operated at a low-angle ($<30°$) (Davis and Lister, 1988; Scott and Lister, 1992; Wernicke, 1995; Foster and John, 1999). These low-angle normal faults are exposed on the flanks of domal core complexes in the central axis of the corridor; these complexes include the Buckskin (Reynolds and Spencer, 1985), Whipple (Davis and Lister, 1988), Chemehuevi (John, 1987) and Sacramento Ranges (Pease and Argent, 1999). The tectonic transport direction across these detachment faults is consistently northeastwards. The footwalls are exhumed terranes of Precambrian basement (metamorphic core complexes) intruded by numerous Cretaceous and Tertiary granitoids and dykes. The hanging walls consist of tilted fault blocks of Tertiary clastic rocks. These clastics often juxtapose footwall mylonites generated at depths that suggest elimination of 10–15 km of crustal thickness across the low-angle detachment (Foster and John, 1999). The sequence of tectonic events is summarised in Table 1.

5.3.1. Depth of origin of the antithetic shears

The initial internal deformation of the currently exposed footwall to the Sacramento Mountains detachment fault changes in style from ductile in the east to brittle in the west (Fig. 8b,c; Pease and Argent, 1999). In the eastern region of the range, the footwall deformation is dominated by a penetrative mylonitic fabric while in the western region of the range, extensional deformation of the footwall is accommodated by brittle fracturing and sub-vertical dyke emplacement (Pease and Argent, 1999). This spatial variation in deformational style of the early structures has been interpreted as an increase in exposed structural depth

(a)

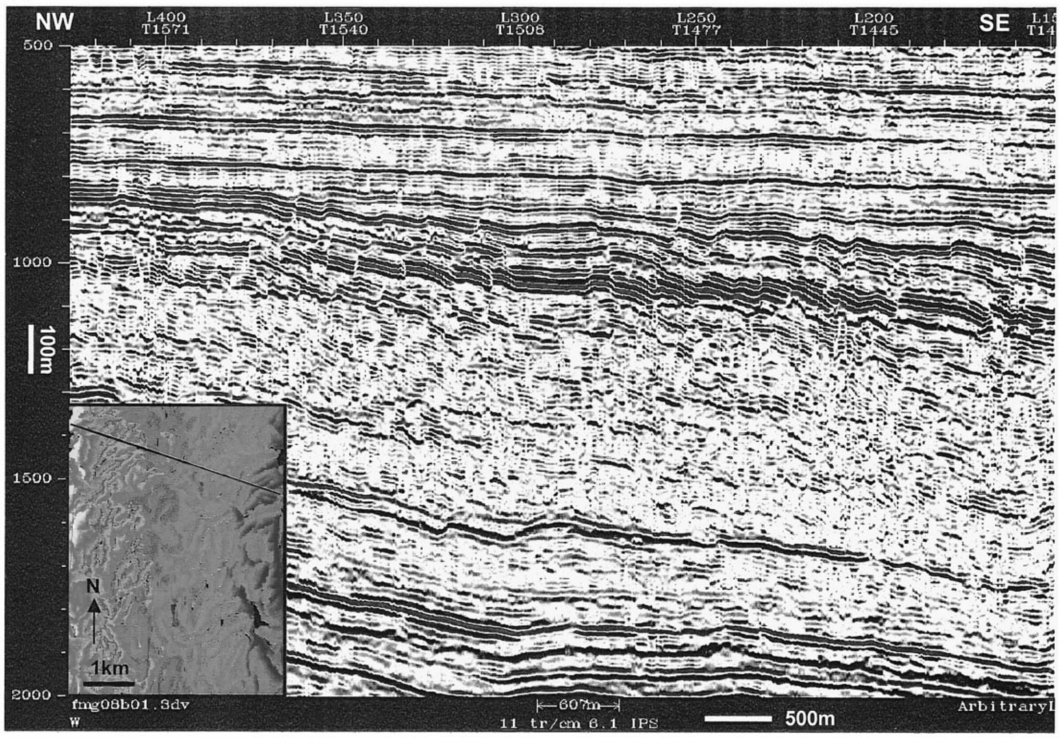

b)

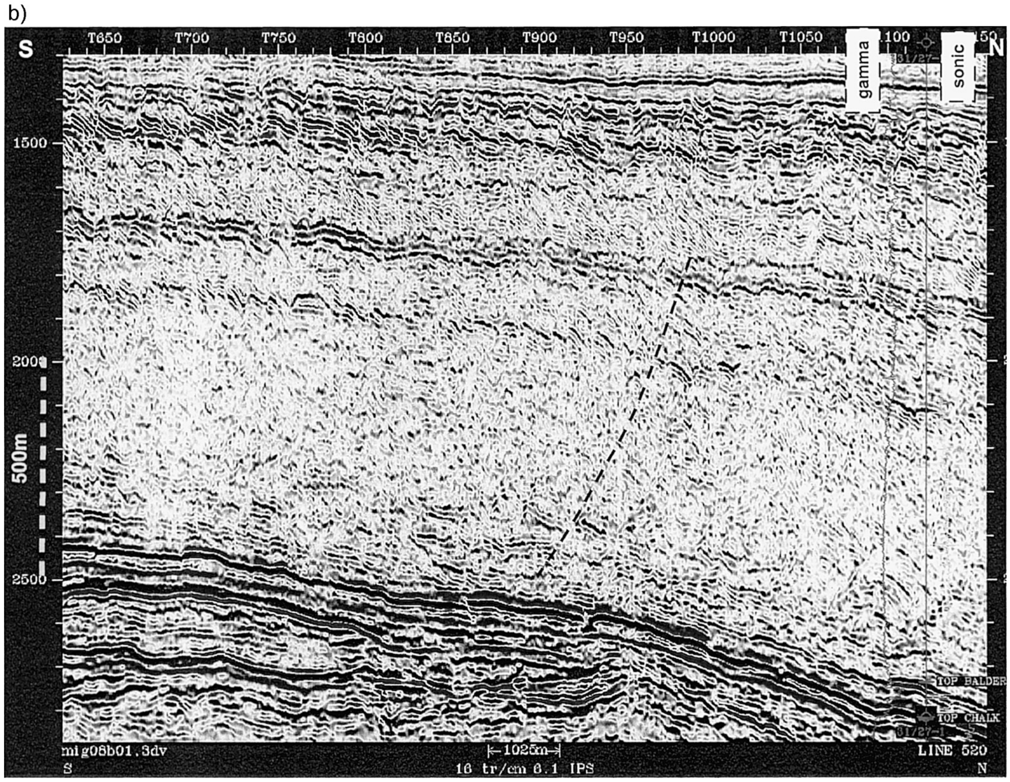

Fig. 6. (a) Antithetic array of domino faults in the Tertiary section on the west side of the Central North Sea. Inset map shows fault pattern mapped on 3D seismic—shading corresponds to two-way time. Vertical exaggeration approximately ×4. (b) Antithetic domino arrays at several stratigraphic levels in the South of the Central North Sea (north flank of the Mid North Sea High). Vertical exaggeration approximately ×6.

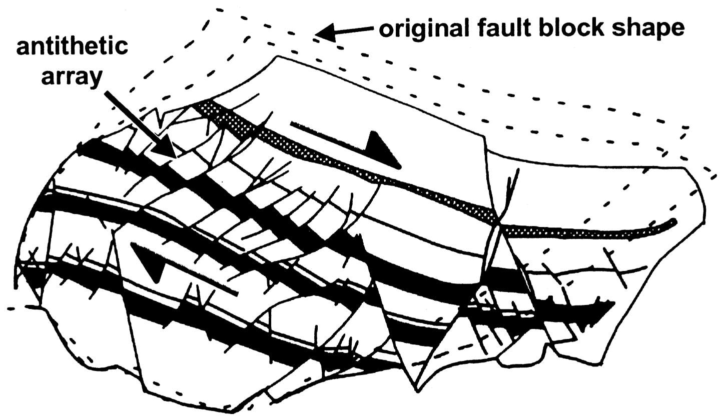

Fig. 7. Antithetic domino array within a deforming fault block, from an analogue model published by Fossen and Gabrielsen (1996). Some of the shear recorded by the changing overall shape of the fault block was accommodated by the domino faulting.

across the footwall 'window' due to progressive downcutting from west to east by the Sacamento Mountains detachment fault (Howard and John, 1987). Between these two distinctive regions of footwall deformation is a domain that represented the Tertiary brittle–ductile transition at the onset of extension (Pease and Argent, 1999). Within this intervening footwall region, discrete shear zones and fractures occur, these are antithetic to the dip and sense of shear of the major low-angle fault zone (Fig. 8d,e).

5.3.2. Geometry of antithetic shears in relation to the low-angle detachment fault

The antithetic shear zones and fractures display consistent present-day dips of 25–35° to the southwest (Fig. 8e; Pease and Argent, 1999). The dominant footwall lithology within this region is a weakly foliated Cretaceous granodiorite. In the Sacramento Mountains this granodiorite is intruded by a two-mica garnet granite that is unfoliated and has yielded a poorly constrained zircon and monazite age of 72 ± 27 Ma (Pease

Table 1
Deformation of the footwall of the Sacramento Mountains metamorphic core complex

Deformation event	Description	References
D4 Post-detachment high-angle faulting	Localised high-angle faulting and strike-slip movement.	Spencer, 1985; Pease and Argent, 1999
D3 Detachment faulting	Miocene aged (~18–14 Ma) low angle detachment faulting with the exhumation of the footwall terrane by tectonic denudation and collapse of the hanging wall. Hanging wall faulting is synthetic to the underlying detachment surface.	Spencer, 1985; Howard and John, 1987; Lister and Davis, 1989; Simpson et al., 1991; Pease and Argent, 1999; Pease et al., 1999
D2 Miocene extension of the footwall	Miocene aged (~20–18 Ma) development of a pervasive upper to middle Greenschist facies mylonitic *LS* foliation in the eastern region of the range, gently dipping to the SW with a top-to-the-northeast sense of shear. The western region of the range is characterised by brittle deformation and the intrusion of E–W striking sub-vertical dykes. Between these two regions is an area dominated by discrete SW dipping extensional shear zones, fractures and dykes intruded within lower greenschist facies conditions. These discrete shear zones are antithetic to the over-riding low-angle detachment fault and have been interpreted as deformation related to extension within the brittle–ductile transition at the initiation of extension.	Spencer, 1985; Howard and John, 1987; Lister and Davis, 1989; Simpson et al., 1991; Pease and Argent, 1999; Pease et al., 1999
D1 Laramide or earlier event	Cretaceous or earlier amphibolite to greenschist facies gneissic foliation, granitic intrusion and associated metamorphism (locally mylonitic). Development of a SW–NW, gently dipping foliation across the range.	Howard and John, 1987; Pease and Argent, 1999

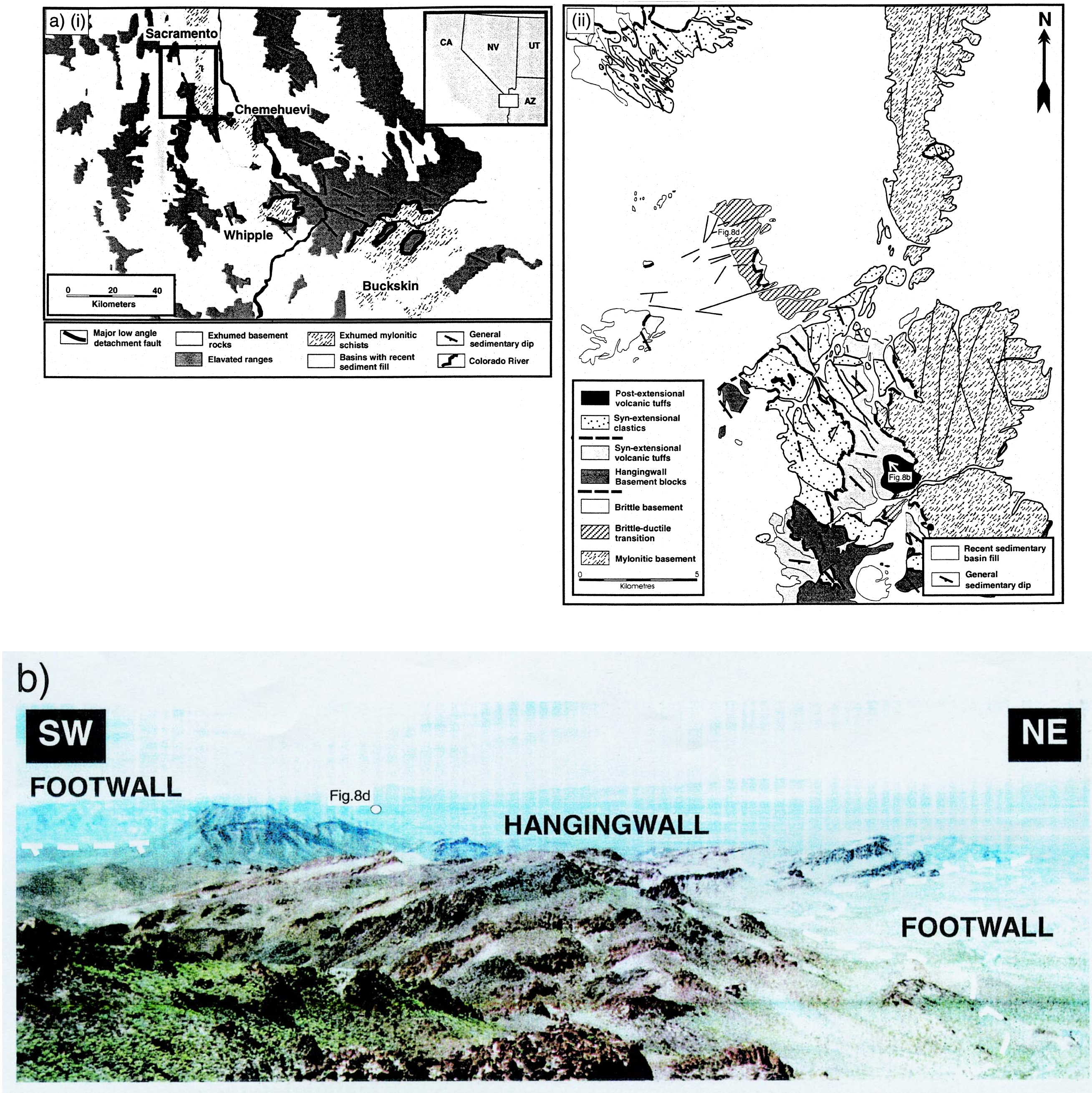

Fig. 8. (a) Location maps for the Basin and Range field example. (b) View north over tilted tuffs and volcaniclastics that lie in the hanging wall to a major, regional low angle detachment. The 'core complexes' in the footwall are labelled. (c) Sketch section at crustal scale after Davis et al. (1986) through the Basin and Range showing how lower crustal rocks can be tectonically exhumed by the low angle detachment and juxtaposed against sedimentary hanging wall sequences. (d) Photograph of footwall rocks from a location interpreted to represent Mid-crustal levels (see text). The outcrop is affected by a number of shears that have a consistent sense of displacement opposite to that of the main detachment. Dykes were synchronous with the shears—both the dykes and shears are truncated by the overlying detachment. (e) Stereonet of antithetic shears data, Sacramento Mountains area. Data in NE quadrant (triangles) are poles to antithetic shears, 692 data, average pole plunges 58/069. Data in SW quadrant are lineations measured on the shear planes, 312 data, average lineation plunges 24/214. (f) Model synthesising the observations made in the vicinity of the Sacramento core complex. (i) 'Antithetic' shears accommodate early, putative top-to-the-northeast shearing; they cut the earliest, Pre-Tertiary sub-horizontal fabric. Dykes are synchronous with the antithetic faults. (ii) Ongoing movement on the antithetic faults shears the dykes and rotates the earliest fabric. The antithetic shears are observed to pin out at outcrop and this system is unable to accommodate large amounts of shear. (iii) A major low-angle detachment cuts the antithetic array and accommodates further movement. A synthetic domino array breaks up the hanging wall of the detachment.

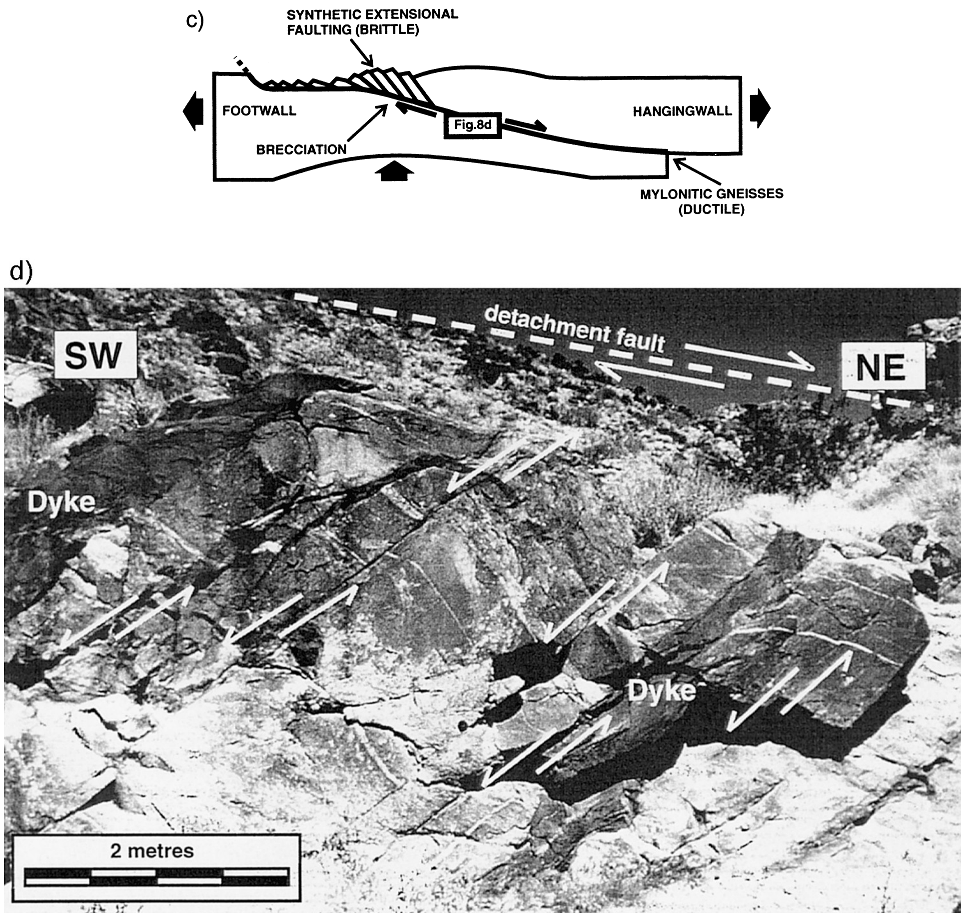

Fig. 8 (*continued*)

et al., 1999). Regionally such granites are Cretaceous in age, intruded prior to Tertiary extension (John, 1987). The pre-existing footwall foliation is offset by the antithetic shear zones. No field evidence was found in this study for an underlying detachment to this antithetic extensional array—the lower fault tips were observed in several instances, hence we interpret that all of the structures in this array 'pin out' with depth.

The antithetic shear zones and fractures do not merge upwards onto the overlying northeasterly dipping detachment fault surface, but are truncated by the detachment fault. Observation of this truncation is not conclusive proof that the antithetic shears pre-date the detachment, as tectonic shaving can modify the initial relationships between a major fault and those that initially splayed from it (Gibbs, 1984; Lister and Davis, 1989).

5.3.3. Radiometric dating of antithetic shears vs. low-angle detachment

The antithetic shears are syntectonically intruded by a suite of dykes (Fig. 8d). Undeformed equivalent dykes in the western region of the field area have a K/Ar biotite age of 19.1 ± 0.2 Ma (Spencer, 1985). Movement on the detachment fault itself is constrained by the presence of tilted volcanic tuffs interbedded within the syntectonic clastic section above the detachment surface dated by a K/Ar biotite age of 17.6 ± 0.2 Ma (Spencer, 1985). The cessation of detachment faulting in the range is constrained by the presence of untilted basalt lavas with K/Ar biotite and sanidine ages of 14.6 ± 0.2 Ma and the extrusion of rhyodacite with a K/Ar age of 14.3 Ma onto the exposed detachment surface at Eagle Peak (Simpson et al., 1991).

5.3.4. Model for role of antithetic shears in evolution of crustal-scale low-angle detachment

There is no doubt that low-angle detachments of regional extent can accommodate significant extension if a suitable detachment 'layer' is initially present (e.g. Trudgill and Cartwright, 1994; Morley and Guerin, 1996). However, detachment faults such as that in the Sacramento mountains described above appear to cut at low angle across various rheological boundaries right through the Earth's crust, including those lithologies at the depth of the brittle–ductile transition, a zone that some consider to be the strongest in a crustal profile (Lister and Davis, 1989). In this context we

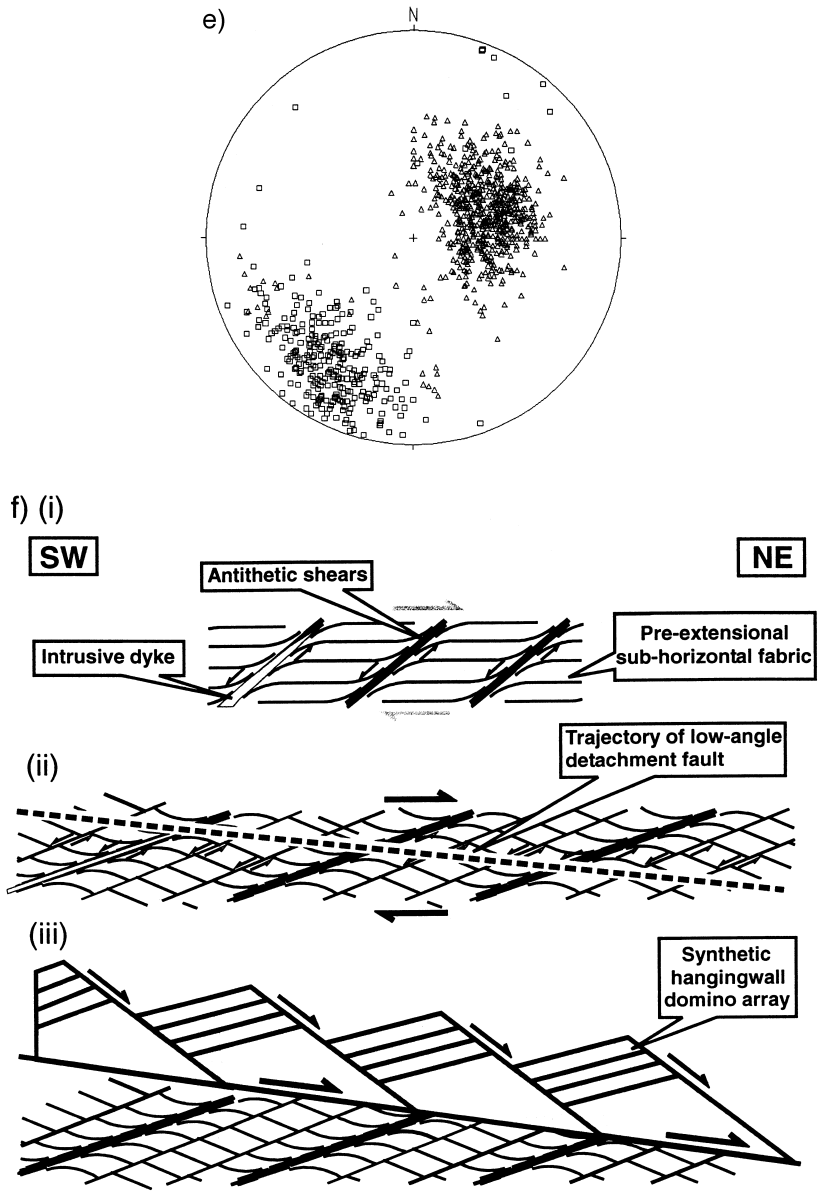

Fig. 8 (*continued*)

note that it is the brittle–ductile transition where the antithetic shears discussed here occur. We propose that these antithetic shears represent the earliest mode of failure at the depth of the brittle–ductile transition, the preferred polarity controlled by incipient top-to-the-northeast shear. The intrusion of these shears by dyke networks illustrates that they represented fluid sinks. Bearing in mind the effects of fluids in terms of reducing the strength of shear zones (e.g. Price and Cosgrove, 1990), the presence of fluid on these shears underlines the potential role of these structures in weakening the mid-crust. We suggest that the mid-crust, weakened in this manner, was prone to shearing, accommodated by the low-angle detachment that linked the brittle upper with the ductile lower crust (c.f. low-angle shear zone propagation across shale layering, Morley and Guerin, 1996). This is one approach to the problem of non-Andersonian propagation of low-angle detachment faults across strong crustal layers (cf. Lister and Davis, 1989; Wernicke, 1995).

The overall sequence of events that appears to have occurred in the Sacramento Mountains core complex based on the field observations and the model described above is shown in Fig. 8(f). Simple shear is initially accommodated at mid-crustal levels by an antithetic fault array, which accommodates very little extension but weakens the brittle–ductile transition zone. Invasion of magma into these shears made this zone particularly weak. Domino rotation of the shears

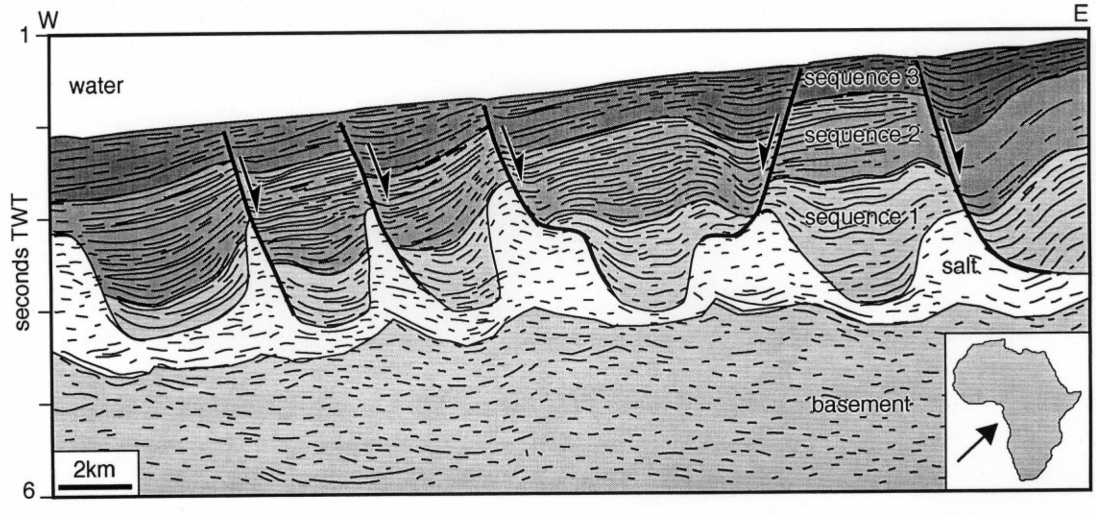

Fig. 9. Domino faults that appear to be antithetic to the regional dip on the passive margin offshore Gabon, after Liro and Coen (1995). Note that 'sequence 1' thickens landward—the possible significance of this in relation to the fault polarity is discussed in the text.

modified their initial dip (Fig. 8f). Regional extension accelerated by means of a through-going, low-angle detachment fault that took advantage of the weakened mid-crust, cutting the antithetic structures. In due course the hanging wall disintegrated into a domino fault array that is synthetic to the regional dip of this detachment and the overall sense of shear. The antithetic structures that pre-date the low-angle detachment at mid-crustal level, and the synthetic domino faults, that are synchronous with the detachment, both fit into the relationship proposed in this paper between fault block boundary conditions and polarity of the faults relative to the overall sense of shear.

6. Discussion of other examples

Many detachments are comprised of intrinsically weak layers, either individual sediment layers as in most of the examples in this paper, or at a crustal scale (Kusznir and Park, 1987). Other detachments cut across existing lithological layering both at a crustal scale (e.g. the Basin and Range low-angle detachments) and in slope failures adjacent to cliffs (fault scarp degradation complexes mentioned below). In all of these cases, the domino fault blocks adhere to the framework outlined in this paper and their hanging walls are characterised by synthetic domino faults.

6.1. Fault scarp collapse

Exposed fault scarps create room for material to slide laterally into, given the presence of suitable detachments. Modification of North Sea Jurassic fault scarps in this manner has been thoroughly reviewed elsewhere (Underhill et al., 1997; Hesthammer and Fossen, 1999), and shown that the so-called 'fault-scarp degradation complexes' are dominated by synthetic faults rooting onto detachment layers in the footwall.

6.2. Oceanic crust

Reviews of fault vergence in oceanic crust reveal an interesting relationship between overall sense of shear, regional dip and dominant fault polarity. Ocean plates adjacent to relatively slow spreading ridges have relatively steep regional dips (Parsons and Sclater, 1977) and are characterised by antithetic polarity of ridge-parallel faults (Carbotte and Macdonald, 1990). On the other hand, plates adjacent to relatively fast spreading centres have lower regional dips and mixed extensional fault polarity populations (Carbotte and Macdonald, 1990; cf. Fig. 1b).

6.3. Gabon

Liro and Coen (1995) illustrate an enigmatic province, offshore Gabon, where faults that are synchronous with the synthetic arrays elsewhere in the west African salt basins, are antithetic to regional dip, yet a salt detachment is known to be present at the base of the fault blocks (Fig. 9). Although this system is kinematically admissible, and indeed has demonstrably been active as an antithetic array during passive margin subsidence, genetic reasons for the updip facing have not been clarified (Liro and Coen, 1995). However, Liro and Coen (1995) also show that the earliest post-salt sequence thickens landward. Employing the relationships proposed here, one would either question the presence of a detachment below the fault blocks (unlikely from the seismic examples presented by Liro and Coen, 1995, although they do not mention well control), or one could propose that the faults were initiated during a pre-rift phase of regional tilt in the opposite direction. Evidence for this putative phase of tilt in the lowermost sequences of the dominoes and in the general understanding of the evolution of the Atlantic rift–pre-rift uplift centred on the trend that ultimately becomes the oceanic rift has been described from several Atlantic margin basins (Withjack et al., 1998).

7. Conclusions

A relationship is proposed between domino fault block boundary conditions (particularly whether or not there is a basal detachment) and polarity of the fault array with respect to the overall sense of shear in the regional dip direction. The relationship is based on several field examples and has not been fully accounted for here, but is underlain by various kinematic and mechanical controls. On the one hand, where no detachment is present in the system, fault arrays appear to be antithetic—in this case, there is a straightforward kinematic selection mechanism as only the antithetic option is in harmony with the overall sense of shear (e.g. as defined by regional tilt of sedimentary layering). On the other hand, if a detachment is present, faults branching from this detachment will tend to be synthetic to the overall sense of shear. The selection mechanism in this case appears to be mechanical and has not been pursued here. Although many natural examples of domino fault arrays have been affected by several phases of post-faulting regional tilt, where evidence can be found to reconstruct vacillations in regional tilt, domino faults appear to adhere to the relationship described above. The relationship appears to be sufficiently consistent for the antithetic/synthetic identification of extensional fault array polarity in relation to the overall sense of shear to be used as an indicator of the absence/presence of basal detachment in the stratigraphy. This represents an instance where the structural style of undrilled areas imaged on seismic data may give an indication of fault block boundary conditions and more importantly the presence or otherwise of significant detachment horizons.

Acknowledgements

The manuscript benefited from reviews by G. Axen and J. Underhill. Fig. 4(c) was prepared by R. Herries. The views expressed here are solely those of the authors and do not necessarily represent those of Amerada Hess Ltd.

References

Axen, G.J., 1988. The geometry of planar domino-style normal faults above a dipping detachment. Journal of Structural Geology 10, 405–411.

Axen, G.J., 1992. Pore pressure, stress increase, and fault weakening in low-angle normal faulting. Journal of Geophysical Research 97, 8979–8991.

Axen, G.J., Bartley, J., 1997. Field tests of the rolling hinge hypothesis. Journal of Geophysical Research 102, 20515–20537.

Brooks, M., Trayner, P.M., Trimble, T.J., 1988. Mesozoic reactivation of Variscan thrusting in the Bristol Channel area. Journal of the Geological Society London 145, 439–444.

Carbotte, S.M., Macdonald, K.C., 1990. Causes of variation in fault-facing direction on the ocean floor. Geology 18, 749–752.

Cartwright, J.A., Lonergan, L., 1996. Volumetric contraction during the compaction of mudrocks: a mechanism for the development of regional-scale polygonal fault systems. Basin Research 8, 183–193.

Childs, C., Easton, S.J., Vendeville, B.C., Jackson, M.P.A., Lin, S.T., Walsh, J.J., Watterson, J., 1993. Kinematic analysis of faults in a physical model of growth faulting above a viscous salt analogue. Tectonophysics 228, 313–329.

Dart, C.J., McClay, K., Hollings, P.N., 1995. 3D analysis of inverted extensional fault systems, southern Bristol Channel basin, UK. In: Buchanan, J.G., Buchanan, P.G. (Eds.), Basin Inversion, Geological Society Special Publication, 88, pp. 393–413.

Davis, G.A., Lister, G.S., 1988. Detachment faulting in continental extension; Perspectives from the Southwestern U.S. Cordillera. In: Clark, S.P. Jr. (Ed.), Processes in Continental Lithospheric Deformation, Geological Society of America Special Paper, 218, pp. 133–159.

Davis, G.A., Lister, G.S., Reynolds, S.J., 1986. Structural evolution of the Whipple and South mountains shear zones, southwestern United States. Geology 14, 7–10.

Davison, I., 1989. Extensional domino fault tectonics: kinematics and geometrical constraints. Annales Tectonicae 3, 12–24.

Diegel, F.A., Karlo, J.F., Schuster, D.C., Shoup, R.C., Tauvers, P.R., 1995. Cenzoic structural evolution and tectono-stratigraphic framework of the northern Gulf coast continental margin. In: Jackson, M.P.A., Roberts, D.G., Snelson, S. (Eds.), Salt Tectonics: A Global Perspective, American Association of Petroleum Geologists Memoir, 65, pp. 109–151.

Duval, B., Cramez, C., Jackson, M.P.A., 1992. Raft tectonics in the Kwanza Basin, Angola. Marine and Petroleum Geology 9, 389–405.

Faure, J.-L., Chermette, J., 1989. Deformation of tilted blocks, consequences on block geometry and extension measurements. Bulletin Societie Geologique France 5, 461–476.

Ferrill, D.A., Morris, A.P., Jones, S.M., Stamatakos, J.A., 1998. Extensional layer-parallel shear and normal faulting. Journal of Structural Geology 20, 355–362.

Fletcher, M.J., Bartley, J.M., Martin, M.W., Glazner, A.F., Walker, J.D., 1995. Large-magnitude continental extension: An example from the Mojave metamorphic core complex. Geological Society of America Bulletin 107, 1469–1483.

Fossen, H., Gabrielsen, R.H., 1996. Experimental modeling of extensional fault systems by use of plaster. Journal of Structural Geology 18, 673–687.

Foster, D.A., John, B.E., 1999. Quantifying tectonic exhumation in an extensional orogen with thermochronology: examples from the southern Basin and Range Province. In: Ring, U., Brandon, M.T., Lister, G.S., Willett, S.D. (Eds.), Exhumation Processes: Normal Faulting, Ductile Flow and Erosion, Geological Society Special Publication, 154, pp. 343–364.

Freund, R., 1974. Kinematics of transform and transcurrent faults. Tectonophysics 21, 93–134.

Gibbs, A.D., 1984. Structural evolution of extensional basin margins. Journal of the Geological Society London 141, 609–620.

Hesthammer, J., Fossen, H., 1998. The use of dipmeter data to constrain the structural geology of the Gullfaks Field, northern North Sea. Marine and Petroleum Geology 15, 549–573.

Hesthammer, J., Fossen, H., 1999. Evolution and geometries of gravitational collapse structures with examples from the Statfjord Field, northern North Sea. Marine and Petroleum Geology 16, 259–281.

Higgs, W.G., Williams, G.D., Powell, C.M., 1991. Evidence for flexural shear folding associated with extensional faults. Geological Society of American Bulletin 103, 710–717.

Higgs, W.G., McClay, K.R., 1993. Analogue sandbox modelling of Miocene extensional faulting in the Outer Moray Firth. In: Williams, G.D., Dobb, A. (Eds.), Tectonics and Seismic Sequence Stratigraphy, Geological Society Special Publication, 71, pp. 141–162.

Horsfield, W.T., 1980. Contemporaneous movement along crossing conjugate normal faults. Journal of Structural Geology 2, 305–310.

Howard, K.A., John, B.E., 1987. Crustal extension along a rooted system of imbricate low-angle faults: Colorado River extensional corridor, California and Arizona. In: Coward, M.P., Dewey, J.F., Hancock, P.L. (Eds.), Continental Extensional Tectonics, Geological Society Special Publication, 28, pp. 299–311.

Jackson, J.A., White, N.J., 1989. Normal faulting in the upper continental crust: observations from regions of active extension. Journal of Structural Geology 11, 15–36.

Jenssen, A.I., Bergslien, D., Rye-Larsen, M., Lindholm, R.M. 1993. Origin of complex mound geometry of Paleocene submarine-fan sandstone reservoirs, Balder field, Norway. In: Parker, J.R. (Ed.), Petroleum Geology of Northwest Europe: Proceedings of the 4th Conference. The Geological Society, pp. 135–143.

John, B.E., 1987. Geometry and evolution of a mid-crustal extensional fault system: Chemehuevi Mountains, southeastern California. In: Coward, M.P., Dewey, J.F., Hancock, P.L. (Eds.), Continental Extensional Tectonics, Geological Society Special Publication, 28, pp. 313–335.

Jordan, P.G., 1991. Development of asymmetric shale pull-aparts in evaporite shear zones. Journal of Structural Geology 13, 399–409.

Kusznir, N.J., Park, R.G., 1987. The extensional strength of the continental lithosphere: its dependence on geothermal gradient, and crustal composition and thickness. In: Coward, M.P., Dewey, J.F., Hancock, P.L. (Eds.), Continental Extensional Tectonics, Geological Society Special Publication, 28, pp. 35–52.

Liro, L.M., Coen, R., 1995. Salt deformation history and postsalt structural trends, offshore southern Gabon, west Africa. In: Jackson, M.P.A., Roberts, D.G., Snelson, S. (Eds.), Salt Tectonics: A Global Perspective, American Association of Petroleum Geologists Memoir, 65, pp. 323–331.

Lister, G.S., Davis, G.A., 1989. The origin of metamorphic core complexes and detachment faults formed during Tertiary continental extension in the northern Colorado River region, U.S.A. Journal of Structural Geology 11, 65–94.

Liu, X., Galloway, W.E., 1997. Quantitative determination of Tertiary sediment supply to the North Sea Basin. American Association of Petroleum Geologists Bulletin 81, 1482–1509.

Mandl, G., 1987. Tectonic deformation by rotating parallel faults: the "bookshelf" mechanism. Tectonophysics 141, 277–316.

Mandl, G., 1988. Mechanics of Tectonic Faulting. Elsevier, Oxford.

Maudit, T., Guerin, G., Brun, J.-P., Lecanu, H., 1997. Raft tectonics: the effects of basal slope angle and sedimentation rate on progressive extension. Journal of Structural Geology 19, 1219–1230.

McClay, K.R., 1990. Extensional fault systems in sedimentary basins: a review of analogue model studies. Marine and Petroleum Geology 7, 206–233.

Mohriak, W.U., Macedo, J.M., Castellani, R.T., Rangel, H.D., Barros, A.Z.N., Latgé, R.J.A., Mizusaki, A.M.P., Szatmari, P., Demercian, L.S., Rizzo, J.G., Aires, J.R., 1995. Salt tectonics and structural styles in the deep-water province of the Cabo Frio region, Rio de Janeiro, Brazil. In: Jackson, M.P.A., Roberts, D.G., Snelson, S. (Eds.), Salt Tectonics: A Global Perspective, American Association of Petroleum Geologists Memoir, 65, pp. 273–304.

Morley, C.K., Guerin, G., 1996. Comparison of gravity-driven deformation styles and behaviour associated with mobile shales and salt. Tectonics 15, 1154–1170.

Naylor, M.A., Mandl, G., Sijpesteijn, C.H.K., 1986. Fault geometries in basement-induced wrench faulting under different initial stress states. Journal of Structural Geology 8, 737–752.

Nur, A., Ron, H., Scotti, O., 1986. Fault mechanics and the kinematics of block rotations. Geology 14, 746–749.

Parsons, B., Sclater, J.G., 1977. An analysis of the variation of ocean floor bathymmetry and heat flow with age. Journal of Geophysical Research 82, 803–827.

Pease, V.L., Argent, J.D., 1999. The Northern Sacramento Mountains, Part I: Structural profile through a crustal shear zone. In: MacNiocaill, C., Ryan, P. (Eds.), Continental Tectonics, Geological Society of London Special Publication, 164, pp. 179–198.

Pease, V.L., Foster, D., O'Sullivan, P., Wooden, J., Argent, J., Fanning, C., 1999. The Northern Sacramento Mountains, Part II: Exhumation history and detachment faulting. In: MacNiocaill, C., Ryan, P. (Eds.), Continental Tectonics, Geological Society of London Special Publication, 164, pp. 199–237.

Price, N.J., Cosgrove, J.W., 1990. Analysis of Geological Structures. Cambridge University Press, Cambridge.

Reynolds, S.J., Spencer, J.E., 1985. Evidence for large-scale transport on the Bullard detachment fault, west-central Arizona. Geology 13, 353–356.

Reynolds, S.J., Lister, G.S., 1990. Folding of mylonitic zones in Cordilleran metamorphic core complexes: Evidence from near the mylonitic front. Geology 18, 216–219.

Scott, R.J., Lister, G.S., 1992. Detachment faults: Evidence for a low-angle origin. Geology 20, 833–836.

Simpson, C., Schweitzer, J., Howard, K.A., 1991. A reinterpretation of the timing, position and significance of part of the Sacramento Mountains detachment. Geological Society of America Bulletin 103, 751–761.

Spencer, J.E., 1985. Miocene low-angle normal faulting and dyke emplacement, Homer Mountain and surrounding areas, southern California and southernmost Nevada. Geological Society of America Bulletin 96, 1140–1155.

Stewart, S.A., Harvey, M.J., Otto, S.C., Weston, P.J., 1996. Influence of salt on fault geometry: examples from the UK salt basins. In: Alsop, G.I., Blundell, D.J., Davison, I. (Eds.), Salt Tectonics. Geological Society Special Publication, 100, pp. 175–202.

Stewart, S.A., Ruffell, A.H., Harvey, M.J., 1997. Relationship between basement-linked and gravity driven fault systems in the UKCS salt basins. Marine and Petroleum Geology 14, 581–604.

Sylvester, A.G., 1988. Strike-slip faults. Geological Society of America Bulletin 100, 1666–1703.

Trudgill, B., Cartwright, J.A., 1994. Relay-ramp forms and normal-fault linkages, Canyonlands National Park, Utah. Geological Society of America Bulletin 106, 1143–1157.

Underhill, J.R., Sawyer, M.J., Hodgson, P., Shallcross, M.D., Gawthorpe, R.L., 1997. Implications of fault scarp degradation for Brent Group prospectivity, Ninian field, Northern North Sea. American Association of Petroleum Geologists Bulletin 81, 999–1022.

Van Wees, J.D., Cloetingh, S., De Vincente, G., 1996. The role of pre-existing faults in basin evolution: constraints from 2D finite element and 3D flexure models. In: Buchanan, P.G., Nieuwland, D.A. (Eds.), Modern Developments in Structural Interpretation, Validation and Modelling. Geological Society Special Publication, 99, pp. 297–320.

Vendeville, B., Cobbold, P.R., Davy, P., Brun, J.P., Choukroune, P., 1987. Physical models of extensional tectonics at various scales. In: Coward, M.P., Dewey, J.F., Hancock, P.L. (Eds.), Continental Extensional Tectonics, Geological Society Special Publication, 28, pp. 95–107.

Walsh, J.J., Watterson, J., Childs, C., Nicol, A., 1996. Ductile strain effects in the analysis of seismic interpretations of normal fault systems. In: Buchanan, P.G., Nieuwland, D.A. (Eds.), Modern Developments in Structural Interpretation, Validation and Modelling. Geological Society Special Publication, 99, pp. 27–40.

Watterson, J., Nicol, A., Walsh, J.J., 1998. Strains at the intersections of synchronous conjugate normal faults. Journal of Structural Geology 20, 363–370.

Wernicke, B., 1995. Low-angle normal faults and seismicity: A review. Journal of Geophysical Research 100, 20159–20174.

Withjack, M.O., Schlische, R.W., Olsen, P.E., 1998. Diachronous rifting, drifting, and inversion on the passive margin of Central Eastern North America: An analog for other passive margins. American Association of Petroleum Geologists Bulletin 82, 817–835.

Woodcock, N.H., Schubert, C. 1994. Continental strike slip tectonics. In: Hancock, P.L. (Ed.), Continental Deformation. Pergamon Press, Oxford, pp. 251–263.